

FINITE ELEMENT MODEL OF ASYMMETRICAL ROTOR-BEARING SYSTEMS

Yang-Gyu Jei* and Chong-Won Lee*

(Received September 10, 1988)

Recently, the finite element method has been successfully used in rotor dynamic analysis. However, the previous works have been restricted to axi-symmetrical rotor-bearing systems. This paper extends the previous finite element modeling to include asymmetrical rotor-bearing systems, consisting of rigid disks, finite shaft elements with distributed mass and elasticity, and discrete bearings. The finite element model developed includes the effects of rotary inertia, gyroscopic moment, transverse shear deformation, internal damping and gravity. The dynamic analysis of multiple shaft rotor-bearing systems modeled by finite element method requires the solution of large order sets of linearized differential equations of motion. To reduce the size of the resulting matrices, the modal transform technique is applied. Finally the accuracy of the finite element model and the modal transform technique is demonstrated.

Key Words: Finite Element Model, Asymmetrical Rotor-Bearing System, Transverse Shear Deformation, Internal Damping, Rotating Coordinates, Whirl Speed, Critical Speed, Forced Vibration

1. INTRODUCTION

The vibrations of asymmetrical rotor-bearing systems have been extensively investigated, but most works have considered only simple models such as a uniform shaft and a single disk mounted on massless shaft (Taylor and Schenectady, 1940, Foote et al., 1943, Dimentberg, 1961, Tondl, 1961, Yamamoto et al. 1968, Ardyfio and Frohrib, 1976). The general method, therefore, for asymmetrical rotor-bearing systems which consist of rigid disks, shaft with distributed mass and elasticity, and discrete bearings is necessary in order to answer to the practical vibration problems.

The transfer matrix method has been a popular numerical method for the analysis of general rotor-bearing systems (Lund and Orcutt, 1967, Lund, 1974). This method has the advantage of small computer memory requirements, but the equations of motion using such a procedure are not explicitly written. In 1980 Inagaki et al. formulated the transfer matrix model for asymmetrical rotor-bearing systems and introduced the Harmonic Balance Method to solve the resulting equation having periodic coefficients. But in their study, the uniformly distributed rotary inertia and gyroscopic effects of the shaft were neglected, and only the major critical speeds and synchronous whirling vibrations near major critical speeds were evaluated.

Recently, the finite element method has been successfully applied to axi-symmetrical rotor-bearing systems (Gasch, 1976, Nelson and McVaugh, 1976, Hashish and Sankar, 1984). Since the system equations of motion derived from the finite element procedure are explicitly written, the additional details such as bearing flexibilities and input excitations can

be easily incorporated in the formulation. And the effects of axial load (Nelson and McVaugh, 1976), internal damping (Zorzi and Nelson, 1977) and shear deformation (Nelson, 1980) can also be considered in finite element formulation. In this paper, a finite element model for asymmetrical rotor-bearing systems is developed in rotating coordinates. The model includes the effects of rotary inertia, gyroscopic moment, transverse shear deformation, internal damping and gravity.

The dynamic analysis of multiple shaft rotor-bearing systems modeled by finite element method requires the solution of large order sets of linearized differential equations of motion. Such large order systems are costly to solve in terms of computer time and storage. Among various matrix reduction techniques (Rouch and Kao, 1980, Glasgow and Nelson, 1980, Kim and Lee, 1986), the modal transform technique (Kim and Lee, 1986) was successfully applied to the axi-symmetrical rotor-bearing system, showing that it can be used to predict whirl speeds and unbalance response with reasonably high accuracy and to provide the reduced computer time and storage requirements. Here the modal transform technique is applied to the asymmetrical rotor-bearing system.

The computer program developed is capable of calculating the major critical speeds, the forward and backward whirl speeds, the corresponding mode shapes, the forced responses, and the instability regions. The accuracy of the finite element model and the sensitivity to the modal truncation are demonstrated.

2. EQUATIONS OF MOTION

One of the advantages of the finite element method resides in its suitability for the automatic formation of the system equations with the separately developed component equations. Since the governing equations of asymmetrical rotor

*Department of Mechanical Engineering, Korea Advanced Institute of Science and Technology, Seoul 130-650, Korea

system in stationary coordinates are of periodically varying coefficients, the governing equations are conveniently expressed in rotating coordinates instead of stationary coordinates. Here the coordinate systems developed in Jei and Lee(1987a) and Jei(1988) are adopted. The S: $oxyz$ triad is a stationary reference fixed on the ground, whereas the R: $OXYZ$ triad is a rotating reference defined relative to the S: $oxyz$ triad by single rotation Ωt about x axis, Ω being spin speed. The body attached coordinates A: $Oabc$ is attached to the cross section with the a axis normal to the cross section. The x , X and a axes are collinear and coincident with the undeformed rotor center line. The deformation of the cross section at an axial distance X are described by the translation $Y(X, t)$ and $Z(X, t)$ in Y and Z directions, respectively, to locate the elastic center line and by the small angular rotation $B(X, t)$ and $\Gamma(X, t)$ about Y and Z directions, respectively, to orient the plane of the cross section. The equations of motion for the rigid disk and the finite shaft element are developed using Lagrangian formulation. The bearing equations are not developed here and only the linearized form of the equations as treated in Lund and Orcutt(1967) and Nelson(1976) is utilized.

2.1 Rigid Disk

The kinetic energy of an axial asymmetrical rigid disk with the mass center coincident with its geometric center is given as

$$T^d = \frac{1}{2} m^d \{ (\dot{Y} - \Omega Z)^2 + (\dot{Z} + \Omega Y)^2 \} + \frac{1}{2} (\rho I_x^d \omega_x^2 + \rho I_y^d \omega_y^2 + \rho I_z^d \omega_z^2) - \rho I_{yz} \omega_y \omega_z \quad (1)$$

where m^d is the mass, ρI_x^d , ρI_y^d , ρI_z^d and ρI_{yz}^d the mass moments of inertia of the rigid disk, and ω_x , ω_y and ω_z the angular rates of the deformed cross section relative to R: $OXYZ$, respectively. Superscript d denotes the rigid disk. Applications of Lagrange's equations yield 4 simultaneous second order differential equations with respect to Y , Z , B and Γ . The resulting linearized equations then become

$$\mathbf{M}^d \ddot{\mathbf{q}}^d + \Omega \mathbf{G}^d \dot{\mathbf{q}}^d - \Omega^2 \mathbf{N}^d \mathbf{q}^d = \mathbf{Q}^d \quad (2)$$

where the terms on the left are related to the relative acceleration, the Coriolis acceleration plus gyroscopic moment, and the centripetal acceleration, respectively. The matrices of \mathbf{M}^d , \mathbf{G}^d , \mathbf{N}^d and \mathbf{q}^d are listed in Appendix A. The generalized force vector \mathbf{Q}^d includes the forces due to the unbalance and the weight of the disk. Notice that, in rotating coordinates, the mass unbalance is constant. For the mass center located at (Y_m^d, Z_m^d) relative to R: $OXYZ$, the force due to the unbalance is

$$\mathbf{Q}_m^d = m^d \Omega^2 \{ Y_m^d \ 0 \ Z_m^d \ 0 \}^T \quad (3)$$

In the horizontal asymmetrical rotor, the force due to the weight of the disk causes, in particular, the second order vibration (Bishop and Parkinson, 1965), i.e.,

$$\mathbf{Q}_g^d = \mathbf{Q}_g^d \cos \Omega t + \mathbf{Q}_g^d \sin \Omega t \quad (4)$$

where

$$\mathbf{Q}_c^d = m^d \mathbf{g} \begin{bmatrix} -1 \\ 0 \\ 0 \\ 0 \end{bmatrix}, \quad \mathbf{Q}_g^d = m^d \mathbf{g} \begin{bmatrix} 0 \\ 0 \\ 1 \\ 0 \end{bmatrix}.$$

The degree of asymmetry of a rigid disk, ϵ^d , is often defined as

$$\epsilon^d = \rho I_x^d / \rho I_y^d \quad (5)$$

where ρI_y^d , ρI_x^d are the moments of inertia about the principal axes of the cross section. When $\epsilon^d = 0$, Eq. (2) becomes identical to Eq. (6) in Nelson and McVaugh(1976) except the selection of the displacement vector.

2.2 Finite Shaft Element

A typical axial asymmetrical shaft element and its coordinates are illustrated in Fig. 1. The finite shaft element here is considered to be the rotating uniform Timoshenko beam which includes transverse shear deformations. The shaft is modeled as an eight degree-of-freedom element with two translations and two rotations at each end of the element. It should be noted that the element cross section displacements (q_1, \dots, q_8) are functions of time and distance, X , along its axis. The rotations (B, Γ) and translations (Y, Z) associated with the bending deformation of the cross-section are related by

$$B(X, t) = \frac{\partial Z_b(X, t)}{\partial X}, \quad \Gamma(X, t) = \frac{\partial Y_b(X, t)}{\partial X} \quad (6)$$

The subscript b is associated with the bending deformation of a Timoshenko beam. The translation of a typical cross-section internal to the element may be represented by

$$\begin{Bmatrix} Y \\ Z \end{Bmatrix} = \mathbf{R} \mathbf{q}^e \quad (7)$$

where the spatial constraint matrix, \mathbf{R} , is given by

$$\mathbf{R} = \begin{bmatrix} r_{y1} & r_{y2} & r_{y3} & r_{y4} & 0 & 0 & 0 & 0 \\ 0 & 0 & 0 & 0 & r_{z1} & r_{z2} & r_{z3} & r_{z4} \end{bmatrix} \quad (8)$$

and

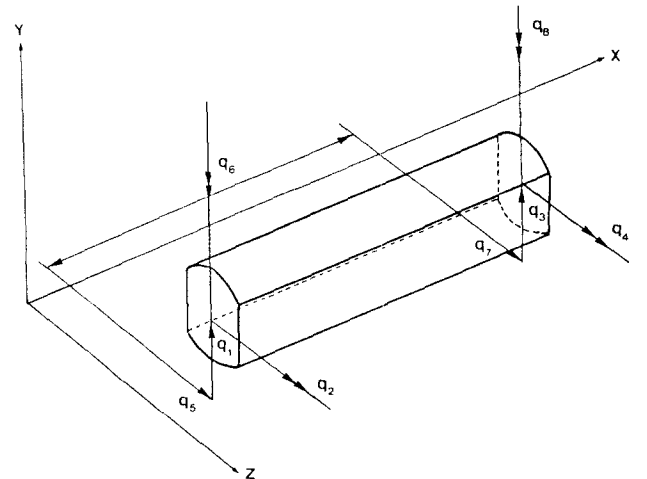


Fig. 1 Coordinates of finite shaft element

$$\mathbf{q}^e = \{q_1, q_2, \dots, q_8\}^T.$$

The rotation can be similarly expressed in the form

$$\begin{Bmatrix} \Gamma \\ B \end{Bmatrix} = \mathbf{C} \mathbf{q}^e \quad (9)$$

where the spatial constraint matrix, \mathbf{C} , is given by

$$\mathbf{C} = \begin{bmatrix} C_{y_1} & C_{y_2} & C_{y_3} & C_{y_4} & 0 & 0 & 0 & 0 \\ 0 & 0 & 0 & 0 & C_{z_1} & C_{z_2} & C_{z_3} & C_{z_4} \end{bmatrix}, \quad (10)$$

The shape functions, r_i and c_i ($i=1, 2, 3, 4$), established by Hashish(1984) for an axi-symmetrical Timoshenko beam element, are employed in this study and provided in Appendix B.

The kinetic energy of the finite shaft element consists of both translational and rotational terms. When the principal axes of the cross section are coincident with the "b" and "c" axes of the body attached coordinates, $Oabc$, the kinetic energy of the differential shaft element located at X then becomes

$$\begin{aligned} dT^e &= \frac{1}{2} \rho A^e \{(\dot{Y} - \Omega Z)^2 + (\dot{Z} + \Omega Y)^2\} dX \\ &+ \frac{1}{2} (\rho I_x^e \omega_x^2 + \rho I_y^e \omega_y^2 + \rho I_z^e \omega_z^2) dX \end{aligned} \quad (11)$$

where ρA^e is the element mass per unit length and ρI_x^e , ρI_y^e and ρI_z^e are the mass moments of inertia of the finite shaft element about (X , Y , Z) axes, respectively. Superscript e denotes the finite shaft element.

The elastic potential energy of the element consists of elastic bending and shear energy. When the principal axes of the cross section are coincident with the "b" and "c" axes of the body attached coordinates, the differential potential energy function then becomes

$$\begin{aligned} dP^e &= \frac{1}{2} \left\{ EI_z \left(\frac{\partial \Gamma}{\partial X} \right)^2 + EI_y \left(\frac{\partial B}{\partial X} \right)^2 \right\} dX \\ &+ \frac{1}{2} k' A^e G \left\{ \left(\frac{\partial Z}{\partial X} - B \right)^2 + \left(\frac{\partial Y}{\partial X} - \Gamma \right)^2 \right\} dX \end{aligned} \quad (12)$$

where k' is the shear form factor and G is the shear modulus. The shear form factor k' is given by 7.8/8.8 for solid circular cross-section shafts, and 13.0/15.3 for solid rectangular cross-section shafts, respectively (Cowper, 1966).

The total kinetic and potential energy is obtained by integrating Eqs. (11) and (12) over the length of the element. By the use of Lagrangian formulation, the equation of motion of a finite shaft element can be obtained as, using Eqs. (7) and (9),

$$\mathbf{M}^e \ddot{\mathbf{q}}^e + \Omega \mathbf{G}^e \dot{\mathbf{q}}^e + (\mathbf{K}^e - \Omega^2 \mathbf{N}^e) \mathbf{q}^e = \mathbf{Q}^e \quad (13)$$

where

$$\mathbf{K}^e = \mathbf{K}_b^e + \mathbf{K}_s^e$$

and the subscript b and s denote the bending and the shear stiffness of a Timoshenko beam, respectively. The symmetric matrices, \mathbf{M}^e and \mathbf{K}^e , and the skew-symmetric matrix, \mathbf{G}^e , are provided in detail in Appendix B. When the principal axes of the cross section are not coincident with "b" and "c"

axes of A: $Oabc$, \mathbf{M}^e , \mathbf{K}^e and \mathbf{G}^e are also provided in Appendix B.

The undamped finite shaft element model of Eq. (13) can be extended to include the linear internal damping. The effects of internal damping may be incorporated into viscous and hysteretic damping forms. The hysteretic damping effect couples the flexural bending moments such that (Lund and Orcutt, 1967, Hashish and Sankar, 1984)

$$\begin{Bmatrix} M_z \\ M_y \end{Bmatrix} = \begin{bmatrix} EI_z \cos \gamma_h & EI_z \sin \gamma_h \\ -EI_y \sin \gamma_h & EI_y \cos \gamma_h \end{bmatrix} \begin{Bmatrix} \Gamma' \\ B' \end{Bmatrix} \quad (14)$$

where the loss angle γ_h is related to the loss factor η_h by

$$\sin \gamma_h = \eta_h / \sqrt{1 + \eta_h^2}.$$

The linear velocity dependent viscous form of internal damping is represented as a simple dashpot model with a damping coefficient η_v . The relationship between bending strain ϵ_x and bending stress σ_x due to internal viscous damping is given by (Zorzi and Nelson, 1980, Özgüven and Özkan, 1984)

$$\sigma_x = \eta_v E \dot{\epsilon}_x. \quad (15)$$

The relationship between the viscous damping and the flexural bending moments becomes

$$\begin{Bmatrix} M_z \\ M_y \end{Bmatrix} = \eta_v \begin{bmatrix} EI_z & 0 \\ 0 & EI_y \end{bmatrix} \begin{Bmatrix} \dot{\Gamma}' \\ \dot{B}' \end{Bmatrix}. \quad (16)$$

Since the angle γ_h is practically very small, the stiffness matrix modification by the factor $\cos \gamma_h$ should not be significant on the rotor behavior. But the nonconservative moments in the off-diagonal terms in Eq. (14) are the significant factor affecting stability. From Eqs. (14) and (16), the differential potential energy and the nonconservative works are given as

$$\begin{aligned} dP^e &= \frac{1}{2} \cos \gamma_h (EI_z \Gamma'^2 + EI_y B'^2) dX \\ dW_{nc} &= - \int_0^l \{ \eta_v (EI_z \dot{\Gamma}' d\Gamma + EI_y \dot{B}' dB') \\ &+ \sin \gamma_h (EI_z B' \delta \Gamma' - EI_y \Gamma' \delta B) \} dX. \end{aligned} \quad (17)$$

The total potential energy of the finite shaft element with a length ℓ are given as, using Eq. (9),

$$P^e = \frac{1}{2} \cos \gamma_h \mathbf{q}^{eT} \mathbf{K}_b^e \mathbf{q}^e. \quad (18)$$

The model expressed by Eq. (18) does not include the effects of transverse shear deformations. The effects of shear deformations can easily be included in the model by replacing the stiffness matrix \mathbf{K}_b^e in Eq. (18) by $\mathbf{K}^e (= \mathbf{K}_b^e + \mathbf{K}_s^e)$ (Özgüven and Özkan, 1984). Using Lagrangian formulation the equation of motion of a finite shaft element including the effects of internal damping and transverse shear deformation can be obtained as

$$\begin{aligned} \mathbf{M}^e \ddot{\mathbf{q}}^e + (\Omega \mathbf{G}^e + \eta_v \mathbf{K}^e) \dot{\mathbf{q}}^e \\ + (\cos \gamma_h \mathbf{K}^e + \sin \gamma_h \mathbf{K}^e \mathbf{S} - \Omega^2 \mathbf{N}^e) \mathbf{q}^e = \mathbf{Q}^e \end{aligned} \quad (19)$$

where $\mathbf{S} = \begin{bmatrix} \mathbf{0} & \mathbf{I} \\ -\mathbf{I} & \mathbf{0} \end{bmatrix}_{8 \times 8}$, and \mathbf{I} is the 4×4 identity matrix. The force vector \mathbf{Q}^e in Eq. (19) includes the forces resulting from

the unbalance and the weight of shaft. For an element with its distributed mass center eccentricity ($Y_m^e(X)$, $Z_m^e(X)$), the equivalent unbalance force, utilizing the consistent matrix approach (Nelson and McVaugh, 1976), is

$$Q_m^e = \int_0^l \rho A^e \Omega^2 \mathbf{R}^T \begin{bmatrix} Y_m^e \\ Z_m^e \end{bmatrix} dX. \quad (20)$$

By assuming a linear distribution of the mass center location along the shaft element, the eccentricity in Y and Z directions for a differential disk located at a distance X can be written as

$$\begin{aligned} Y_m^e(X) &= Y_m^e(0) \left(1 - \frac{X}{\ell}\right) + Y_m^e(\ell) \frac{X}{\ell} \\ Z_m^e(X) &= Z_m^e(0) \left(1 - \frac{X}{\ell}\right) + Z_m^e(\ell) \frac{X}{\ell}. \end{aligned} \quad (21)$$

The equivalent forces in Eq. (20) are presented in Appendix B. The force resulting from the shaft weight with distributed mass are, in rotating coordinates,

$$Q_g^e(X, t) = Q_c^e(X) \cos \Omega t + Q_s^e(X) \sin \Omega t \quad (22)$$

where

$$\begin{aligned} Q_c^e(X) &= \frac{1}{2} \rho A^e \ell g \{-1, 0, -1, 0, 0, 0, 0, 0\}^T \\ Q_s^e(X) &= \frac{1}{2} \rho A^e \ell g \{0, 0, 0, 0, 1, 0, 1, 0\}^T. \end{aligned}$$

The gravity force causes the second order vibration. Here the degree of asymmetry of finite shaft element is defined as

$$\varepsilon^e = \rho I_x^e / \rho I_y^e \quad (23)$$

where ρI_y^e and ρI_x^e are the mass moments of inertia of the finite shaft element about the principal axes of the cross section.

2.3 Bearings

The equation of motion of an isotropic bearing as it whirls about its steady state position is assumed to be represented, in rotating coordinates, by

$$\mathbf{C}^b \dot{\mathbf{q}}^b + (\mathbf{K}^b + \Omega \mathbf{D}^b) \mathbf{q}^b = \mathbf{Q}^b \quad (24)$$

where

$$\begin{aligned} \mathbf{C}^b &= \begin{bmatrix} c & c_{yz} \\ -c_{yz} & c \end{bmatrix}, \quad \mathbf{K}^b = \begin{bmatrix} k & k_{yz} \\ -k_{yz} & k \end{bmatrix} \\ \mathbf{D}^b &= \begin{bmatrix} c_{yz} & -c \\ c & c_{yz} \end{bmatrix}, \quad \mathbf{q}^b = \{Y, Z\}^T \end{aligned}$$

and $k (= k_{yy} = k_{zz})$, $k_{yz} (= -k_{zy})$, $c (= c_{yy} = c_{zz})$ and $c_{yz} (= -c_{zy})$ are the spring and damping coefficients of the isotropic bearing, respectively. Superscript b denotes the bearing. For anisotropic bearings, Eq. (24) will contain periodic coefficients, resulting in parametrically excited equation of motion.

3. SYSTEM EQUATION

The assembled system equation of motion in rotating

coordinates, consisting of component equations of (4), (19) and (24), is of the form

$$\mathbf{M}^s \ddot{\mathbf{q}}^s + (\mathbf{C}^s + \Omega \mathbf{G}^s) \dot{\mathbf{q}}^s + (\mathbf{K}^s + \Omega \mathbf{D}^s - \Omega^2 \mathbf{N}^s) \mathbf{q}^s = \mathbf{Q} \quad (25)$$

where

$$\begin{aligned} \mathbf{M}^s &= \begin{bmatrix} m_{yy} & m_{yz} \\ m_{yz}^T & m_{zz} \end{bmatrix}_{N \times N}, & \mathbf{C}^s &= \begin{bmatrix} c_{yy} & c_{yz} \\ c_{yz} & c_{zz} \end{bmatrix}_{N \times N} \\ \mathbf{G}^s &= \begin{bmatrix} 0 & -g_{yz} \\ g_{yz}^T & 0 \end{bmatrix}_{N \times N}, & \mathbf{K}^s &= \begin{bmatrix} k_{yy} & k_{yz} \\ k_{yz} & k_{zz} \end{bmatrix}_{N \times N} \\ \mathbf{D}^s &= \begin{bmatrix} c_{yz}^b & -c^b \\ c^b & c_{yz}^b \end{bmatrix}_{N \times N}, & \mathbf{N}^s &= \begin{bmatrix} n_{yy} & n_{yz} \\ n_{yz}^T & n_{zz} \end{bmatrix}_{N \times N} \\ \mathbf{q}^s &= \{\mathbf{q}_y^s, \mathbf{q}_z^s\}_{N \times 1}, & \mathbf{Q} &= \{\mathbf{Q}_y^s, \mathbf{Q}_z^s\}_{N \times 1}. \end{aligned}$$

The whirl speed at given speed can be determined by solving the eigenvalue problem associated with the homogeneous part of Eq. (25). For computational purpose, the homogeneous part of Eq. (25) is often rewritten in the first order state vector form

$$\dot{\mathbf{h}} = \mathbf{A} \mathbf{h} \quad (26)$$

where

$$\begin{aligned} \mathbf{A} &= \begin{bmatrix} -\mathbf{M}^{s-1}(\mathbf{C}^s + \Omega \mathbf{G}^s) & -\mathbf{M}^{s-1}(\mathbf{K}^s + \Omega \mathbf{D}^s - \Omega^2 \mathbf{N}^s) \\ \mathbf{I} & \mathbf{0} \end{bmatrix}, \\ \mathbf{h} &= \{\dot{\mathbf{q}}^s, \mathbf{q}^s\}^T. \end{aligned}$$

For an assumed solution form, $\mathbf{h} = \mathbf{h}_o e^{\lambda t}$, the associated eigenvalue problem becomes

$$(\mathbf{A} - \lambda \mathbf{I}) \mathbf{h}_o = \mathbf{0}. \quad (27)$$

The eigenvalues are normally found in the form

$$\lambda_r = \delta_r + j\omega_r \quad (28)$$

where ω_r is the whirl speed relative to rotating coordinates. The complex conjugates of Eq. (28) also become the eigenvalues of Eq. (27). Therefore the whirl speeds referred to stationary coordinates are given as

$$\pm \omega_r + \Omega, \quad (29)$$

When the damping is negligibly small, the eigenvalue becomes a pure imaginary, that is, $\lambda_r = j\omega_r$. If $\omega_r = \sigma \Omega$, where σ is the whirl ratio, Eq. (25) can be rewritten as

$$[\Omega^2 (\sigma^2 \mathbf{M}^s - j\sigma \mathbf{G}^s + \mathbf{N}^s) - \mathbf{K}^s] \mathbf{q}_o^s = \mathbf{0}. \quad (30)$$

The eigenvalue problem of Eq. (30) gives undamped whirl speeds along the given whirl ratio σ .

4. MODAL TRANSFORM

The eigenvalue problem of Eq. (25), when the dampings, gyroscopic moments and the cross coupled terms of mass and stiffness matrices are not considered, becomes the simple eigenvalue problem of the form

$$m_{yy} \ddot{\mathbf{q}}_y^s + (k_{yy} - \Omega^2 m_{yy}) \mathbf{q}_y^s = \mathbf{0} \quad (31a)$$

$$\mathbf{m}_{zz}\ddot{\mathbf{q}}_z^s + (\mathbf{k}_{zz} - \Omega^2 \mathbf{m}_{zz}) \mathbf{q}_z^s = 0. \quad (31b)$$

From the simple eigenvalue problems of Eqs. (31a) and (31b), the lowest r eigenvalues and the corresponding real eigenvectors are easily obtained, satisfying the orthogonality conditions

$$\begin{aligned} \phi_y^T \mathbf{m}_{yy} \phi_y &= \mathbf{I}_{r \times r} \\ \phi_y^T (\mathbf{k}_{yy} - \Omega^2 \mathbf{m}_{yy}) \phi_y &= \lambda_{y \ r \times r} \\ \phi_z^T \mathbf{m}_{zz} \phi_z &= \mathbf{I}_{r \times r} \\ \phi_z^T (\mathbf{k}_{zz} - \Omega^2 \mathbf{m}_{zz}) \phi_z &= \lambda_{z \ r \times r}. \end{aligned} \quad (32)$$

Let us define the transformation matrix $\phi_{N \times 2r}$ such as

$$\mathbf{q}^s = \phi \xi^s \quad (33)$$

where

$$\phi = \begin{bmatrix} \phi_{yy} & \mathbf{0} \\ \mathbf{0} & \phi_{zz} \end{bmatrix}$$

and ξ^s is the $2r \times 1$ reduced state vector. Substituting Eq. (33) into Eq. (25) and premultiplying by ϕ^T yields

$$\mathbf{m}^s \ddot{\xi}^s + \mathbf{c}^s \dot{\xi}^s + \mathbf{k}^s \xi^s = \phi^T \mathbf{Q}^s \quad (34)$$

where

$$\begin{aligned} \mathbf{m}^s &= \phi^T \mathbf{M}^s \phi, \quad \mathbf{c}^s = \phi^T (\mathbf{C}^s + \Omega \mathbf{G}^s) \phi \\ \mathbf{k}^s &= \phi^T (\mathbf{K}^s + \Omega \mathbf{D}^s - \Omega^2 \mathbf{N}^s) \phi. \end{aligned}$$

Eq. (34) is the reduced order dynamic equation approximately representing the lowest $2r$ modes of the general asymmetrical rotor-bearing system. To evaluate the whirl speeds and mode shapes for various spin speeds, the new transformation matrix has to be evaluated for each spin speed because of the presence of the spin speed dependent coefficients in Eq. (31). But the transformation matrix for a given spin speed can be used as the Ritz basis vector for the neighboring spin speeds without causing severe errors. For the some increment of spin speed, $\Delta \Omega$, to the given spin speed, Ω_o , the new eigenvalue problem at $\Omega_o + \Delta \Omega$ may be constructed as, with fair accuracy,

$$\mathbf{m}^s \ddot{\xi}^s + (\mathbf{c}^s + \Delta \mathbf{c}^s) \dot{\xi}^s + (\mathbf{k}^s + \Delta \mathbf{k}^s) \xi^s = 0 \quad (35)$$

where

$$\begin{aligned} \Delta \mathbf{c}^s &= \Delta \Omega \phi^T \mathbf{G}^s \phi, \\ \Delta \mathbf{k}^s &= \phi^T [\Delta \Omega \mathbf{D}^s - (\Delta \Omega^2 + 2 \Delta \Omega \Omega_o) \mathbf{N}^s] \phi \end{aligned}$$

and ϕ is the transformation matrix evaluated at the spin speed Ω_o .

5. FORCED VIBRATIONS

The forced vibrations of an asymmetrical rotor system with isotropic bearings are often caused by the small defects such as the initial bend and lack of mass balance that are inevitably present in any rotors and the weight of the rotor itself. Since the force due to unbalance is a constant relative to rotating coordinates, the unbalance response is also a constant relative to rotating coordinates. From Eq. (25) the

unbalance response is given by

$$\mathbf{q}_m^s = (\mathbf{K}^s + \Omega \mathbf{D}^s - \Omega^2 \mathbf{N}^s)^{-1} \mathbf{Q}_m^s. \quad (36)$$

The static force developed by gravity bends the asymmetrical rotor system twice per revolution so that the corresponding response attains the significant amplitude at about half the major critical speeds. In rotating coordinates, the force due to the weight of the rotor is of the form

$$\mathbf{Q}_m^s = \mathbf{Q}_m^s \cos \Omega t + \mathbf{Q}_m^s \sin \Omega t \quad (37)$$

Thus the steady state response due to rotor weight may be expressed as

$$\mathbf{q}_m^s = \mathbf{q}_m^s \cos \Omega t + \mathbf{q}_m^s \sin \Omega t. \quad (38)$$

Substitution of Eq. (38) into Eq. (25) yields

$$\mathbf{q}^c = [(\mathbf{K}^s + \Omega \mathbf{D}^s - \Omega^2 \mathbf{N}^s - \Omega^2 \mathbf{M}^s) - j \Omega \mathbf{C}^s]^{-1} \mathbf{Q}^c \quad (39)$$

where

$$\mathbf{q}^c = \mathbf{q}^s + j \mathbf{q}_s^s, \quad \mathbf{Q}^c = \mathbf{Q}^s + j \mathbf{Q}_s^s.$$

From Eqs. (36) and (39) the forced response is then described by

$$\mathbf{q}^s = \mathbf{q}_m^s + \mathbf{q}_c^s \cos \Omega t + \mathbf{q}_s^s \sin \Omega t. \quad (40)$$

The displacement of the rotor, \mathbf{q}^s , in rotating coordinates can be easily expressed in stationary coordinates by using the orthogonal transformation.

6. NUMERICAL EXAMPLES

In order to demonstrate the accuracy of the finite element model, a uniform asymmetrical shaft supported by isotropic bearings at both ends is considered to determine the whirl speeds and major critical speeds. The data for the simulation is taken as follows:

$$\begin{aligned} \ell &= 1.5 \text{ m}, \quad I_y = 0.8482 \times 10^{-5} \text{ (m}^4\text{)}, \\ I_z &= 0.1188 \times 10^{-4} \text{ (m}^4\text{)}, \quad A = 0.01131 \text{ (m}^2\text{)}, \\ \rho &= 7806.0 \text{ kg/m}^3, \quad E = 2.078 \times 10^{11} \text{ N/m}^2, \\ k^0 &= 0.2089 \times 10^8 \text{ (N/m)} \text{ at } x=0 \\ k^l &= 0.4178 \times 10^8 \text{ (N/m)} \text{ at } x=l \end{aligned}$$

The exact solutions are obtained by the analytical method which treats the rotor system as a distributed parameter system whose motions are described by partial differential equations (Jei and Lee, 1987a). The system is modeled by five finite shaft segments and two discrete bearings. The shear deformations are not considered in this case. When the spin speed is 15000rpm, the whirl speeds relative to rotating coordinates, ω_r , are given in Table 1. The whirl speeds referred to stationary coordinates can be obtained by using the relation of Eq. (29).

At the major critical speeds where the whirl speeds coincide with the spin speeds, the whirl speed, ω_r , relative to rotating coordinates vanishes. It is necessary, therefore, to assume a solution $\mathbf{q}^s = \mathbf{q}_c^s = \text{constant}$ to obtain the major critical speeds. The resulting eigenvalue problem is

Table 1 Whirl speeds (RPM) of an uniform shaft supported by isotropic bearings

Exact	F.E.M.	Error (%)
4599.67	4594.84	0.105
5090.49	5111.91	0.421
10402.4	10402.0	0.004
19552.5	19552.8	0.002
25178.8	25190.4	0.046
27090.4	27225.6	0.499
34733.2	34751.1	0.052
56420.1	56557.5	0.244

Table 2 Critical speeds (RPM) of an uniform shaft supported by isotropic bearings

Exact	F.E.M.	Error (%)
4367.88	4368.14	0.006
4722.96	4723.19	0.005
10268.9	10272.1	0.031
10582.7	10585.3	0.025
19385.2	19405.4	0.104
21229.7	21248.6	0.089
40161.6	40312.8	0.376
47011.0	47184.5	0.369

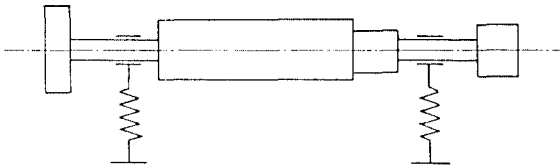


Fig. 2 General asymmetrical rotor system

$$(K^s - Q^2 N^s) q_0^s = 0, \quad (41)$$

The major critical speeds of the uniform shaft are given in Table 2. As shown in Tables 1 and 2, the results well coincide with the exact results obtained by the analytical solution method (Jei and Lee, 1987a, Jei, 1988).

In order to illustrate the effectiveness of the finite element method developed here for general asymmetrical rotor-bearing systems, a typical system as shown in Fig. 2 is considered. The system model consists of seven shaft seg-

Table 3 Asymmetrical rotor configuration data

Material properties				
$E = 2.078 \times 10^{11} \text{N/m}^2$,		$\rho = 7806.0 \text{kg/m}^3$		
Symmetrical shaft element				
Element	Length(m)	Radius(m)		
1	0.26	0.05		
2	0.20	0.05		
5	0.20	0.75		
6	0.16	0.05		
7	0.30	0.05		
Asymmetrical shaft element				
Element	Length(m)	$I_y (\text{m}^4)$	$I_z (\text{m}^4)$	
3	0.44	0.6545×10^{-4}	0.9163×10^{-4}	
4	0.44	0.6545×10^{-4}	0.9163×10^{-4}	
Rigid disk				
Location	Mass(kg)	$\rho I_x (\text{kg m}^2)$	$\rho I_y (\text{kg m}^2)$	$\rho I_z (\text{kg m}^2)$
1	196.2	3.9237	2.6158	2.6158
8	55.18	0.6207	0.3564	0.3564
Bearing				
Node	$k_{yy} = k_{zz} (\text{N/m})$	$C_{yy} = C_{zz} (\text{N sec/m})$		
2	0.33×10^8	0.18×10^4		
7	0.33×10^8	0.18×10^4		

ments, two rigid disks and two discrete bearings. The shear deformations are considered in this case. The system configuration data are listed in Table 3. Since the modes for the use of the basis vectors of modal transform are obtained without considering the velocity dependent coefficient, $C^s + QG^s$, the modal transform using the lowest r modes as basis vectors causes the modal truncation errors. When the spin speed, Ω , is 20000 rpm, Table 4 shows the damped whirl speeds and logarithmic decrement, defined as $-2\pi\delta_r/\omega_r$, in rotating coordinates with the various levels of modal truncations. As shown in Table 4, the modal truncation errors rapidly converge to zero as the number of used modes increases. The undamped whirl speeds obtained using Eq. (30) are shown in Fig. 3. The lowest 6 modes are used for the modal transform. As discussed in Jei and Lee(1987b) the curve veerings in the eigenvalue occur as shown in Fig. 3. The undamped major critical speeds of this system are given in Table 5.

Table 4 Whirl speeds of the multiple shaft rotor-bearing systems in rotating coordinates

Full ($r=14$)		$r=10$	$r=8$
3133.55/0.1604E+0		3113.48/0.1604E+0	3113.47/0.1605E+0
12989.1 /0.1097E-3		12988.9 /0.1124E-3	12986.9 /0.1612E-3
15543.7 /0.2842E-1		15544.1 /0.2840E-1	15549.3 /0.2762E-1
16048.1 /0.1516E-1		16047.9 /0.1517E-1	16047.7 /0.1515E-1
17229.8 /0.7069E-2		17229.8 /0.7070E-2	17229.6 /0.7055E-2
21739.8 /0.8733E-3		21740.0 /0.8733E-3	21744.3 /0.8652E-3
23388.6 /0.7736E-2		23388.6 /0.7737E-2	23390.2 /0.7799E-2
23890.1 /0.6500E-2		23890.5 /0.6515E-2	23897.8 /0.6479E-2
24742.7 /0.3460E-1		24744.2 /0.3460E-1	24748.7 /0.3416E-1
$r=6$		$r=4$	$r=2$
3112.03/0.1609E+0		3075.59/0.1581E+0	
12923.8 /0.4004E-3		12613.5 /0.2560E-3	
15663.3 /0.2434E-1		15957.7 /0.1568E-1	15942.2/0.1642E-1
16036.5 /0.1507E-1			
17228.3 /0.7033E-2		17107.8 /0.7924E-2	17100.8/0.8165E-2
21767.1 /0.8841E-3		22835.7 /0.5638E-2	22854.3/0.5978E-2
23401.9 /0.7923E-2		23873.4 /0.9756E-2	23920.3/0.1063E-1
24102.5 /0.7076E-2			

(RPM)

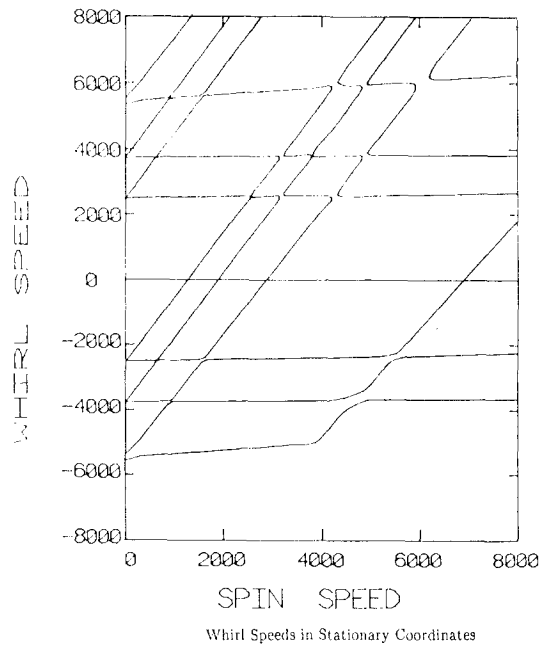


Fig. 3 Whirl speeds of general asymmetrical rotor system

Table 5 Undamped major critical speeds

1.	2555.86
2.	2558.07
3.	3792.10
4.	3802.38
5.	5920.83
6.	6198.84
7.	16079.3
8.	16390.5

(RPM)

7. CONCLUSIONS

A finite element model for general asymmetrical rotor-bearing systems is developed in rotating coordinates. The model includes the effects of rotary inertia, gyroscopic moment, transverse shear deformation, internal damping and gravity. To reduce the size of the matrices resulting from the finite element modeling of rotor-bearing systems, the modal transform technique is applied. The simulation results show that whirl speeds and major critical speeds can be accurately estimated by the use of the developed finite element model. It is also shown that the modal transform technique can be used to predict whirl speeds with fair accuracy, providing the reduced computer time and storage requirements.

REFERENCES

- Ardayfio, D. and Frohrib, D.A., 1976, "Instabilities of an Asymmetric Rotor With Asymmetric Shaft Mounted on Symmetric Elastic Supports", *J. of Eng. for Industry*, pp. 1161~1165.
- Bishop, R.E.D and Parkinson, A.G., 1965, "Second Order Vibration of Flexible Shafts", *Phil. Trans. of Royal Society of London*, Vol. 259, pp. 1~31.
- Cowper, G.R., 1966, "The shear Coefficient in Timoshenko'

s Beam Theory", *J. of Applied Mechanics*, pp. 335~340.

Dimentberg, F.M., 1961, "Flexural Vibration of Rotating Shaft", translated from Russian by Production Engineering Research Association, Butterworths, London.

Foote, W.R., Ponitsky, H. and Slade, J.J. Jr, 1943, "Critical Speeds of a Rotor With Unequal Flexibilities, Mounted in Bearings of Unequal Flexibility", *J. of Applied Mechanics*, pp. A77~A84.

Gasch, R., 1976, "Vibration of Large Turbo-Rotors in Fluid-Film Bearings on an Elastic Foundation", *J. of Sound and Vibration*, Vol. 47, No. 1, pp. 53~73.

Glasgow, D.A. and Nelson, H.D., 1980, "Stability Analysis of Rotor-Bearing System Using Component Mode Synthesis", *J. of Mechanical Design*, pp. 352~359.

Hashish, E. and Sankar, T.S., 1984, "Finite Element and Modal Analysis of Rotor-bearing Under Stochastic Loading Conditions", *J. of Vibration, Acoustics, Stress, and Reliability in Design*, pp. 80~89.

Inagaki, T., Kanki, H. and Shirahi, K., 1980, "Response Analysis of a General Asymmetrical Rotor-bearing System", *J. of Eng. for Industry*, pp. 147~157.

Jei, Y.G. and Lee, C.W., 1987, "Modal Analysis of Asymmetrical Rotor-Bearing System", presented at KSME Meeting, Dynamics and Control Division, August.

Jei, Y.G. and Lee, C.W., 1987, "On Curve Veering In the Eigenvalue Problem of Rotor-Bearing System", presented at KSME Meeting.

Jei, Y.G., 1988, "Vibrations of Continuous Asymmetrical Rotor-Bearing Systems", Ph. D. Thesis.

Kim, Y.D. and Lee, C.W., 1986, "Finite Element Analysis of Rotor-Bearing Systems using Modal Transform", *J. of Sound and Vibration*, Vol. 111, pp. 441~456.

Lund, J.W. and Orcutt, F.K., 1967, "Calculations and Experiments on the Unbalance of a Flexible Rotor", *J. of Eng. for Ind.*, Vol. 39, No. 4, pp. 785~796.

Lund, J.W., 1974, "Stability and Damped Critical Speeds of a Flexible Rotor in Fluid-Film Bearings", *J. of Eng. for Industry*, 1974, pp. 509~517.

Nelson, H.D. and McVaugh, J.M., 1976, "The Dynamics of Rotor-bearing systems Using Finite Elements", *J. of Eng. for Industry*, pp. 593~600.

Nelson, H.D., 1980, "A Finite Rotating Shaft Element Using Timoshenko Beam Theory", *J. of Mech. Design*, pp. 793~803.

Özguven, H.N. and Özkan, Z.L., 1984, "Whirl Speeds and Unbalance Response of Multibearing Rotors Using Finite Elements", *J. of Vib., Acoustics, Stress, and Reliability in Design*, 1984, Vol. 106, pp. 72~79.

Rouch, K.E. and Kao, J.S., 1980, "Dynamic Reduction in Rotor Dynamics by the Finite Element Method", *J. of Mechanical Design*, pp. 360~368.

Taylor, H.D. and Schenectady, N.Y., 1940, "Critical-Speed Behavior of Unsymmetrical Shafts", *J. of Applied Mechanics*, pp. A71~A79.

Tondl, A., 1965, "Some Problems of Rotor Dynamics, London", Chapman and Hall, Ltd.

Yamamoto, T., Ota, H. and Kono, K., 1968, "On the Unstable Vibration of a Shaft With Unsymmetrical Stiffness Carrying an Unsymmetrical Rotor", *J. of Applied Mechanics*, pp. 313~321.

Zorzi, E.S. and Nelson, H.D., 1977, "Finite Element Simulation of Rotor-bearing Systems with Internal Damping", *J. of Eng. for Power*, pp. 71~76.

APPENDIX

A. Element Matrices of Rigid Disk

$$\mathbf{M}^d = \begin{bmatrix} m^d & 0 & 0 & 0 \\ 0 & \rho I_z^d & 0 & \rho I_{yz}^d \\ 0 & 0 & m^d & 0 \\ 0 & \rho I_{yz}^d & 0 & \rho I_y^d \end{bmatrix},$$

$$\mathbf{N}^d = \begin{bmatrix} m^d & 0 & 0 & 0 \\ 0 & \rho I_y^d - \rho I_x^d & 0 & -\rho I_{yz}^d \\ 0 & 0 & m^d & 0 \\ 0 & -\rho I_{yz}^d & 0 & \rho I_z^d - \rho I_x^d \end{bmatrix},$$

$$\mathbf{G}^d = \begin{bmatrix} 0 & 0 & -2m^d & 0 \\ 0 & 0 & 0 & \rho I_o^d \\ 2m^d & 0 & 0 & 0 \\ 0 & -\rho I_o^d & 0 & 0 \end{bmatrix},$$

$$\rho I_o^d = \rho I_x^d - \rho I_y^d - \rho I_z^d,$$

$$\mathbf{q}^d = \{Y, \Gamma, Z, B\}^T$$

B. Shape Functions and Element Matrices of Shaft Element

Since the shaft is asymmetric in stiffness, the transverse shear effect of each principal plane is different. The transverse shear effect in OXY plane is $\varphi_z = \frac{12EI_z}{k'AG\ell^2}$, and the transverse shear effect in OXZ plane is $\varphi_y = \frac{12EI_y}{k'AG\ell^2}$.

Shape Functions

(1) Shape Functions for Translations

$$r_{y_i}(X)|_{\varphi=\varphi_z}, \quad r_{z_i}(X)|_{\varphi=\varphi_y} = \frac{1}{1+\varphi} [r_{bi}(X) + \varphi r_{si}(X)]$$

where

$$r_{b_1} = 1 - 3\left(\frac{X}{\ell}\right)^2 + 2\left(\frac{X}{\ell}\right)^3, \quad r_{s_1} = 1 - \left(\frac{X}{\ell}\right)$$

$$r_{b_2} = X\left(1 - 2\left(\frac{X}{\ell}\right) + \left(\frac{X}{\ell}\right)^2\right), \quad r_{s_2} = \frac{X}{2}\left(1 - \left(\frac{X}{\ell}\right)\right)$$

$$r_{b_3} = 3\left(\frac{X}{\ell}\right)^2 - 2\left(\frac{X}{\ell}\right)^3, \quad r_{s_3} = \left(\frac{X}{\ell}\right)$$

$$r_{b_4} = \ell\left(-\left(\frac{X}{\ell}\right)^2 + \left(\frac{X}{\ell}\right)^3\right), \quad r_{s_4} = \frac{X}{2}\left(-1 + \left(\frac{X}{\ell}\right)\right)$$

(2) Shape Functions for Rotations

$$c_{y_i}(X)|_{\varphi=\varphi_z}, \quad c_{z_i}(X)|_{\varphi=\varphi_y} = \frac{1}{1+\varphi} [c_{bi}(X) + \varphi c_{si}(X)]$$

where

$$c_{b_1} = \frac{6}{\ell}\left(\left(\frac{X}{\ell}\right)^2 - \left(\frac{X}{\ell}\right)\right), \quad c_{s_1} = 0$$

$$c_{b_2} = 1 - 4\left(\frac{X}{\ell}\right) + 3\left(\frac{X}{\ell}\right)^2, \quad c_{s_2} = 1 - \left(\frac{X}{\ell}\right)$$

$$c_{b_3} = \frac{6}{\ell}\left(-\left(\frac{X}{\ell}\right)^2 + \left(\frac{X}{\ell}\right)\right), \quad c_{s_3} = 0$$

$$c_{b_4} = 3\left(\frac{X}{\ell}\right)^2 - 2\left(\frac{X}{\ell}\right), \quad c_{s_4} = \left(\frac{X}{\ell}\right)$$

and the subscripts b and s denote the bending and shear deformations of a Timoshenko beam, respectively.

Element Matrices of Finite Shaft Element

The equation of the finite shaft element can be written as follows:

$$\mathbf{M}^e \ddot{\mathbf{q}}^e + \mathcal{Q} \mathbf{G}^e \dot{\mathbf{q}}^e + (\mathbf{K}^e - \mathcal{Q}^2 \mathbf{N}^e) \mathbf{q}^e = \mathbf{Q}^e \quad (\text{B-1})$$

where

$$\mathbf{M}^e = \begin{bmatrix} \mathbf{a}_1 + \rho I_z^e \mathbf{a}_4 & \mathbf{0} \\ \mathbf{0} & \mathbf{k}_2 + \rho I_y^e \mathbf{k}_3 \end{bmatrix}_{8 \times 8},$$

$$\mathbf{G}^e = \begin{bmatrix} \mathbf{0} & -2\rho A \mathbf{a}_5^T \\ 2\rho A \mathbf{a}_5 & \mathbf{0} \end{bmatrix}_{8 \times 8},$$

$$\mathbf{K}^e = \begin{bmatrix} EI_z \mathbf{b}_1 & \mathbf{0} \\ \mathbf{0} & EI_y \mathbf{b}_2 \end{bmatrix}_{8 \times 8},$$

$$\mathbf{N}^e = \begin{bmatrix} \rho A^e \mathbf{a}_1 - \rho I_z^e \mathbf{a}_4 & \mathbf{0} \\ \mathbf{0} & \rho A^e \mathbf{a}_2 - \rho I_y^e \mathbf{a}_3 \end{bmatrix}_{8 \times 8}$$

When the principal axes of the cross section are not coincident with the "b" and "c" axes of the body attached coordinates, $Oabc$, Eq. (B-1) is transformed as

$$\mathbf{Q}^T \mathbf{M}^e \mathbf{Q} \ddot{\mathbf{q}}^e + \mathcal{Q} \mathbf{Q}^T \mathbf{G}^e \mathbf{Q} \dot{\mathbf{q}}^e + \mathbf{Q}^T (\mathbf{K}^e - \mathcal{Q}^2 \mathbf{N}^e) \mathbf{Q} \mathbf{q}^e = \mathbf{Q}^T \mathbf{Q}^e \quad (\text{B-2})$$

where the orthogonal transformation matrix \mathbf{Q} is given as

$$\mathbf{Q} = \begin{bmatrix} \mathbf{I} \cos \theta & -\mathbf{I} \sin \theta \\ \mathbf{I} \sin \theta & \mathbf{I} \cos \theta \end{bmatrix} \quad (\text{B-3})$$

where \mathbf{I} is the 4×4 identity matrix, and θ is the relative orientation angle between the principal axes of the cross section and the "b" and "c" axes of the body attached coordinates.

The element matrices of Eq. (B-1) are given as follows;

$$\mathbf{a}_1|_{\varphi=\varphi_z}, \quad \mathbf{a}_2|_{\varphi=\varphi_y} = \frac{\ell}{420(1+\varphi)^2} (\mathbf{a}_{12}^0 + \varphi \mathbf{a}_{12}^1 + \varphi^2 \mathbf{a}_{12}^2)$$

where

$$\mathbf{a}_{12}^0 = \begin{bmatrix} 156 & 22\ell & 54 & -13\ell \\ & 4\ell^2 & 13\ell & -3\ell^2 \\ \text{sym} & & 156 & -22\ell \\ & & & 4\ell^2 \end{bmatrix}$$

$$\mathbf{a}_{12}^1 = \begin{bmatrix} 294 & 38.5\ell & 126 & -31.5\ell \\ & 7\ell^2 & 31.5\ell & -7\ell^2 \\ \text{sym} & & 294 & -38.5\ell \\ & & & 7\ell^2 \end{bmatrix}$$

$$\mathbf{a}_{12}^2 = \begin{bmatrix} 140 & 17.5\ell & 70 & -17.5\ell \\ & 3.5\ell^2 & 17.5\ell & -3.5\ell^2 \\ \text{sym} & & 140 & -17.5\ell \\ & & & 3.5\ell^2 \end{bmatrix}$$

and

$$\mathbf{a}_3|_{\varphi=\varphi_y}, \quad \mathbf{a}_4|_{\varphi=\varphi_z} = \frac{\ell}{30(1+\varphi)^2} (\mathbf{a}_{34}^0 + \varphi \mathbf{a}_{34}^1 + \varphi^2 \mathbf{a}_{34}^2)$$

where

$$\mathbf{a}_{34}^0 = \begin{bmatrix} 36 & 3\ell & -36 & 3\ell \\ & 4\ell^2 & -3\ell & -\ell^2 \\ \text{sym} & & 36 & -3\ell \\ & & & 4\ell^2 \end{bmatrix}$$

$$\mathbf{a}_{34}^1 = \begin{bmatrix} 0 & -15\ell & 0 & -15\ell \\ & 5\ell^2 & 15\ell & -5\ell^2 \\ \text{sym} & & 0 & 15\ell \\ & & & 5\ell^2 \end{bmatrix}$$

$$\mathbf{a}_{34}^2 = \begin{bmatrix} 0 & 0 & 0 & 0 \\ & 10\ell^2 & 0 & 5\ell^2 \\ \text{sym} & & 0 & 0 \\ & & & 10\ell^2 \end{bmatrix}$$

and

$$\mathbf{a}_5 = \frac{\ell}{420(1+\varphi_y)(1+\varphi_z)} (\mathbf{a}_5^0 + \varphi_y \mathbf{a}_5^1 + \varphi_z \mathbf{a}_5^1{}^T + \varphi_y \varphi_z \mathbf{a}_5^2)$$

where

$$\mathbf{a}_5^0 = \mathbf{a}_{12}^0, \quad \mathbf{a}_5^2 = \mathbf{a}_{12}^2$$

$$\mathbf{a}_5^1 = \begin{bmatrix} 147 & 21\ell & 63 & -14\ell \\ 17.5 & 3.5\ell^2 & 17.5\ell & -3.5\ell^2 \\ 63 & 14\ell & 147 & -21\ell \\ -17.5\ell & -3.5\ell^2 & -17.5\ell & 3.5\ell^2 \end{bmatrix}$$

and

$$\mathbf{b}_{1|\varphi=\varphi_z}, \quad \mathbf{b}_{2|\varphi=\varphi_y} = \frac{\ell}{(1+\varphi)^2} (\mathbf{b}_{12}^0 + \varphi \mathbf{b}_{12}^1)$$

where

$$\mathbf{b}_{12}^0 = \begin{bmatrix} 12 & 6\ell & -12 & 6\ell \\ & 4\ell^2 & -6\ell & 2\ell^2 \\ \text{sym} & & 12 & -6\ell^2 \\ & & & 4\ell^2 \end{bmatrix}$$

$$\mathbf{b}_{12}^1 = \begin{bmatrix} 0 & 0 & 0 & 0 \\ & \ell^2 & 0 & -\ell^2 \\ \text{sym} & & 0 & 0 \\ & & & \ell^2 \end{bmatrix}$$

and the equivalent unbalance force

$$\mathbf{Q}_m^e = \frac{\rho A^e \Omega^2}{1+\varphi_y} \begin{bmatrix} Y_m(0) \left(\frac{7}{20} + \varphi_z \frac{1}{3} \right) + Y_m(\ell) \left(\frac{3}{20} + \varphi_z \frac{1}{6} \right) \\ Y_m(0) \left(\frac{\ell}{20} + \varphi_z \frac{\ell}{24} \right) + Y_m(\ell) \left(\frac{\ell}{30} + \varphi_z \frac{\ell}{24} \right) \\ Y_m(0) \left(\frac{2}{30} + \varphi_z \frac{1}{6} \right) + Y_m(\ell) \left(\frac{7}{20} + \varphi_z \frac{1}{3} \right) \\ - Y_m(0) \left(\frac{\ell}{5} + \varphi_z \frac{\ell}{24} \right) - Y_m(\ell) \left(\frac{\ell}{20} + \varphi_z \frac{\ell}{24} \right) \\ Z_m(0) \left(\frac{7}{20} + \varphi_y \frac{1}{3} \right) + Z_m(\ell) \left(\frac{3}{20} + \varphi_y \frac{1}{6} \right) \\ Z_m(0) \left(\frac{\ell}{20} + \varphi_y \frac{\ell}{24} \right) + Z_m(\ell) \left(\frac{\ell}{30} + \varphi_y \frac{\ell}{24} \right) \\ Z_m(0) \left(\frac{3}{20} + \varphi_y \frac{1}{6} \right) + Z_m(\ell) \left(\frac{7}{20} + \varphi_y \frac{1}{3} \right) \\ - Z_m(0) \left(\frac{\ell}{5} + \varphi_y \frac{\ell}{24} \right) - Z_m(\ell) \left(\frac{\ell}{20} + \varphi_y \frac{\ell}{24} \right) \end{bmatrix}$$